

1
2
3 **Chemical ozone loss and chlorine activation in the Antarctic winters**
4 **2013–2020**

5
6 R. Roy^{1,2*}, P. Kumar¹, J. Kuttippurath^{1*}, F. Lefevre³
7

8 ¹*CORAL, Indian Institute of Technology Kharagpur, Kharagpur–721302, India.*

9 ²*Department of Physical Oceanography, Cochin University of Science and Technology, Kochi, India.*

10 ³*LATMOS/IPSL, Sorbonne Université, UVSQ, CNRS, Paris, France*

11
12 *Correspondence to:* R. Roy and J. Kuttippurath (rainaroy2105@gmail.com; jayan@coral.iitkgp.ac.in)
13

14 **Abstract**

15 The annual formation of an ozone hole in the austral spring has regional and global climate implications. Antarctic
16 ozone hole has already changed the precipitation, temperature and atmospheric circulation patterns, and thus, the
17 surface climate of many regions in the Southern Hemisphere (SH). Therefore, the study of ozone loss variability is
18 important to assess its consequential effects on the climate and public health. Our study uses satellite observations
19 (the Microwave Limb Sounder on Aura) and the passive tracer method to quantify the ozone loss for the past eight
20 years (2013–2020) in the Antarctic. We observe the highest ozone loss (about 3.5 ppmv) in 2020, owing to the high
21 chlorine activation (about 2.2 ppbv), steady polar vortex, and huge expanses of polar stratospheric clouds (PSCs)
22 (12.6 million km²). The spring of 2019 also showed a high ozone loss, although the year had a rare minor warming
23 in mid-September. The chlorine activation in 2015 (1.9 ppbv) was the weakest, and the wave forcing from the
24 lower latitudes was very high in 2017 (up to -60 Kms⁻¹). The analysis shows significant interannual variability in
25 the Antarctic ozone as compared to the immediate previous decade (2000–2010). The study helps to understand
26 the role of dynamics and chemistry in the interannual variability of ozone depletion over the years.

27 **Keywords:** Antarctic; Ozone loss estimates; Polar Vortex; climate Change; Model simulations

28 **Short title:** Antarctic ozone loss in 2013–2020
29
30
31

33 **Introduction**

34

35 An important event in the Antarctic stratosphere during the austral spring that has caught global attention ever since
36 its discovery in the 1980s is the Antarctic ozone hole (Farman et al., 1985). The chlorine free radicals released from
37 the chlorofluorocarbons (CFCs) and other ozone-depleting substances (ODSs) activate the catalytic cycles that led
38 to severe ozone loss (e.g., Stolarski and Cicerone, 1974; Rowland et al., 1976). The extreme cold conditions that
39 prevail in the poles facilitate the formation of Polar Stratospheric Clouds (PSCs), which serve as the activation
40 surface for the ODSs. Apart from these, the relatively stable Antarctic polar vortex also contributes significantly to
41 the formation of ozone holes annually (Solomon et al., 2014). Since the discovery of ODSs in the 1970s from
42 anthropogenic activities, ozone loss has continued to rise and reached its worst phase in the late 1980s and early
43 1990s (e.g., WMO, 2014). The growth of ODSs was curtailed after the enactment of the Montreal Protocol in 1987.
44 Ratifying the environmental treaty led to a stabilisation of the ozone loss from the late 1990s to the early 2000s in
45 the Antarctic. Despite this, there was no significant increase in total column ozone during those times (e.g.,
46 Weatherhead et al., 2000; WMO, 2007; Angell et al., 2009). Beyond 2000, significant recovery trends in the lower
47 stratospheric ozone were presented with evidence from both ground and satellite observations (e.g., Yang et al.,
48 2008; Salby et al., 2011; Solomon et al., 2016; Chipperfield et al., 2017; Kuttippurath and Nair, 2017; de Laat et
49 al., 2017; Pazmiño et al., 2018; Wespes et al., 2019; Johnson et al., 2023). A reduction in the saturation of ozone
50 loss over the period 2001–2017 was also observed in the Antarctic, confirming the positive ozone trends in the
51 region (Kuttippurath et al., 2018).

52 Here, we present the long-term analysis of ozone loss for the winters 2013–2020 considering the chemical and
53 dynamical characteristics of the winters. Although a few of the years have been studied individually, the long-term
54 analysis helps in better understanding the evolution of the winters (e.g., WMO, 2015; Krummel et al., 2016;
55 Wargan et al., 2020; Manney et al., 2020; Klekociuk et al., 2021). The dynamics of these winters are studied using
56 different meteorological parameters. The study offers a high-resolution analysis of the interannual variability of
57 ozone at various altitudes using the data obtained from the Aura Microwave Limb Sounder (MLS) (Froidevaux et
58 al., 2008; Santee et al., 2008). The ozone loss is calculated using the passive tracer simulated by the REPROBUS
59 (Reactive Processes Ruling the Ozone Budget in the Stratosphere) chemical transport model (CTM) (Lefèvre et al.,
60 1994). Therefore, we use a single dataset and the same method to estimate ozone loss for all eight years to assess
61 the interannual variability, which would make the comparisons among the winters meaningful and coherent.

62 **Data and Methods**

63

64 We have analysed the meteorology of the winters from 2013 to 2020 using the Modern-Era Retrospective Analysis
65 for Research and Applications (MERRA-2) data (Gelaro et al., 2017). MERRA 2 data are available for 42 pressure
66 levels at a spatial resolution of $0.5^\circ \times 0.625^\circ$. The nature of austral springs is studied by the polar cap temperature
67 zonally averaged between 60° and 90° S at 100 hPa, the minimum polar cap temperature at 10 hPa, the area of
68 polar stratospheric clouds at 460 K, and the mean heat flux averaged over the latitude band 45° – 75° S. The PSC
69 area is estimated using the amount of water vapour of 5 ppm and nitric acid of 4.97 ppt at 460 K. Besides, the
70 MERRA 2 dataset is also employed to analyse the vertical evolution of temperature averaged at 60° – 90° S.

71 The ozone loss is estimated using the passive tracer method (Kuttippurath et al., 2015). The tracer is simulated by
72 the REPROBUS CTM, which is identical to ozone, but without interactive chemistry. It is a three-dimensional
73 model driven by the European Centre for Medium-Range Weather Forecasts (ECMWF) operational analyses. The
74 analysis is performed for the altitude range of 1000–0.01 hPa (137 levels). In the model, the advection is performed
75 by the winds on the hybrid sigma-pressure coordinates, and the trace gases are advected by a semi-lagrangian
76 technique (Williamson and Rasch, 1989). In our study, the passive tracer is initialised on June 1 of each year and
77 continued until the end of November. The loss is then computed by subtracting the measured ozone from the
78 modelled passive ozone, which is also called measured or observed ozone loss. Note that the model simulations
79 are used only for the passive ozone in this study. Since the tracer initialisation for recent years was made 1 April
80 2020, there was a consequential offset in the tracer values with respect to other years on 1st of June. This offset is
81 corrected for the ozone loss computation for the year 2020. The loss in each day is estimated inside the polar vortex
82 as it is more prevalent there, and thus, the polar vortex edge is calculated using the equivalent latitude (Nash et al.,
83 1996; Müller et al., 2005). The measurements of ozone and chlorine monoxide (ClO) are taken from the MLS
84 version 4.2. These ozone data have a vertical resolution of 2–3 km, a vertical range of 261–0.02 hPa and an accuracy
85 of 0.1–0.4 ppmv. The ClO measurements are performed at 640 GHz, and these data have a vertical resolution of
86 3–3.5 km at 147–1 hPa with an accuracy of about 0.2–0.4 ppbv. These ClO measurements have a latitude-dependent
87 bias of around 0.2–0.4 ppbv, depending on vertical height (Livesey et al., 2013).

88

89

90 **Results and Discussion**

91 **Meteorology of the winters**

92 Fig. 1 shows the meteorology of the winters as illustrated with the polar cap temperature (60–90° S) at 100 hPa, the minimum temperature averaged over 50°–90° S at 100 hPa, PSC area at 460 K and the heat flux averaged between 45° and 75° S at 100 hPa. The top panel shows the mean temperature (60°–90° S) at 100 hPa, and the coloured lines represent individual years. Temperature decreases from the beginning of winter (June) onwards and reaches its lowest in August. The lowest temperature for most years is observed in August, but it continued to September in 2015 and 2020. Temperature is in the order of 195–208 K during this period in most years (Fig. 1). In the years 2013, 2014, 2015, and 2020, the temperature shows below 195 K (the PSC formation threshold). However, the temperature shows a sudden rise from late August (202 K) to mid-September (218 K) in 2019, indicative of the occurrence of a Sudden Stratospheric Warming (SSW). This event has been reported in some of the previous studies and has been described as a minor Warming (mW) (e.g., Shen et al., 2020a,b; Yamazaki et al., 2020; Roy et al., 2022). Temperature in August 2017 is also higher than that in previous years but lower than in 2019. There is a rise in temperature at the beginning of the austral spring. However, temperatures persist below 195 K during early September 2015. The lowest temperatures range during the winter–spring period are found in 2015 and 2020, as depicted in Fig. 1.

108 Fig. 1 (second panel from top) shows the minimum polar cap temperature for each winter, and is lower than the PSC formation threshold (195 K). This continues in the early spring for all years except in 2019, and the minimum value rises soon after and is higher than 195 K in the late spring. The minimum temperature reaches this threshold for most days and thus, the ideal conditions for the formation of PSCs are found in all winters. Therefore, the PSC area has grown since the beginning of winter and is highest in August (up to 28 million km²). Corresponding to the periods of longest duration of minimum temperature, PSCs persist until early November in 2015, 2018 and 2020, but are relatively short-lived in 2017 and 2019. As the mean temperature peaks in early to mid-September 2019, the PSC area drops and diminishes by late September. However, they dissipated by mid-October in 2017.

116 A major factor affecting the strength of the polar vortex is tropospheric forcing. The strength of this forcing is highly reduced in the Antarctic, except for a few winters. According to Zuev et al. (2019), the strengthening of the Antarctic polar vortex in winter and spring is due to the seasonal temperature variations in the subtropical lower stratosphere. Fig. 1 (bottom) shows the tropospheric forcing estimated for all years. The heat flux averaged between the adjacent mid-latitude and higher latitudes is found to be directed southward, particularly in late winter and early

121 spring. The years 2019 and 2017 are characterised by very strong wave forcing, as shown by the high flux values
122 (from -40 to -50 Kms⁻¹). Klekociuk et al. (2020) reported that the easterly phase of QBO favoured the enhanced
123 wave activity in 2017; a reason for the relatively higher temperature in that winter. Milinevsky et al. (2019) and
124 Evtushevsky et al. (2020) also find similar results for both winters. The zonal average of heat flux stays between -
125 30 and 10 Kms⁻¹ for most winters, and the flux increases as the spring approaches. However, these forcings are
126 limited in the years 2015 and 2020.

127 **Temporal evolution of temperature with altitude**

128 Fig. 2 shows the temporal evolution of zonal mean (60°–90° S) temperature profiles in the Antarctic for the years
129 2013–2020. The coloured contours show the temperature across the seasons and white contour lines represent 188,
130 195 and 210 K. Here, the zonal winds (westerlies) are overlaid with black contours, and the easterlies are in red. In
131 general, temperature increases towards the end of spring in the stratosphere, but it started to rise in the lower
132 stratosphere much earlier during the spring in 2019 and 2017. Temperature contours of 250–265 K extend to
133 slightly below 10 hPa and there is a slight reduction in the speed of westerlies during the period. Temperatures
134 below 195 K are found in the lower stratosphere (100–70 hPa) until mid-October in 2015 and 2020. Similarly, the
135 area covered by 195 K was also moderately large in 2013, 2014, 2016 and 2018. However, this is lowest in 2019
136 and relatively very small in 2017. The appearance of easterlies below 10 hPa is late (end of November) and thus
137 the vortex lasted longer in 2015 and 2020, whereas as early as late October in 2017 and 2019. We also made an
138 assessment inside the vortex, to examine the consistency of our analysis with and without the vortex criterion (see
139 Figure S1). The key features are same in both analyses, such as the very low temperatures in the lower stratosphere,
140 strong easterlies and late appearance of easterlies in the middle stratosphere in 2015 and 2020, the early appearance
141 and minor warming in 2019, and large and extended period of PSC threshold temperature (195 K) in 2018. Since
142 the meteorology is different inside the vortex, small differences in the temperature (e.g., PSC threshold area) and
143 wind (middle stratospheric westerlies in 2015 and 2020) values are also found between the two.

144 **Ozone, chlorine activation and ozone loss**

145 Fig. 3 shows the temporal evolution of ozone (in ppmv) inside the vortex deduced from the MLS data for the period
146 2013–2020. The ozone concentration reduces in the lower altitudes every year as time progresses (mainly in spring),
147 as illustrated in Fig. 3. It is observed from previous studies that the ozone loss is maximum in the lower stratosphere
148 in all years (Solomon et al., 1999). Contrary to this, ozone increases in the upper stratosphere as the winter

149 progresses towards spring. Ozone in the lower stratosphere (400–600 K) is around 0.1–3 ppmv in 2013, 2014,
150 2015, 2016, 2018 and 2020. Unlike in the cold winters, ozone is slightly higher (by 0.5–1.5 ppmv) in the lowermost
151 stratosphere in 2019. Similarly, ozone in the lower stratosphere (400–450 K) is higher than in the previous cold
152 years in 2017, owing to the higher temperature there. The lowest ozone for the altitude range of 400–475 K is
153 observed in 2015, 2018 and 2020, in which the 0.5 ppmv contour extends to 475–500 K.

154

155 Figure 4 presents the temporal evolution of ClO (right) and ozone loss (left) at different altitudes during the period
156 of study. Since there are unreasonably high tracer values in June due to initialisation problem, the ozone loss is not
157 calculated for 10 June 2018 and 20 July 2019. In general, ozone loss is highest at 400–550 K (lower stratosphere)
158 during September and October in all years. The loss is smaller than 1.4 ppmv in the upper stratosphere, mostly
159 driven by the NO_x-based chemistry (e.g., Kuttippurath et al., 2015). The loss in 2014 and 2015 is almost similar,
160 about 2.6–3.0 ppmv at the peak ozone loss altitude (450–550 K) during September and October. The loss in 2013
161 reaches up to 3.0 ppmv by mid-October and is higher than in 2014, 2015, 2017 and 2018 (e.g., Vargin et al., 2020).
162 The ozone loss reported by Strahan et al. (2018) for 2015 is similar to the very cold winters in Antarctica and is
163 slightly higher than our estimate for that winter. The ozone loss with altitude is larger in 2015 than other winters
164 (see Fig. 4). The preconditioning for ozone loss in 2013 and 2014 was ensured by high chlorine activation at the
165 same altitude range (Kuttippurath et al., 2015). Among these three years (2013–2015), before the period of highest
166 ozone loss, chlorine activation reaches its peak values in August and September. ClO amounts up to 2.2 ppbv in
167 2013 and 2014, and 2.0 ppbv in 2015 during this period. This high chlorine activation lasted for almost a month at
168 the peak ozone loss altitude (450–550 K) in 2013, but for a shorter duration in 2014 and 2015. Similar values for
169 ozone loss and ClO (1.8–2.2 ppbv) are also estimated for 2017 and 2018, and the highest ClO stayed intact for 15–
170 20 days before attaining the maximum ozone loss.

171

172 The ozone loss in 2016 is about 3–3.2 ppmv in September and 3.4 ppmv in October. Note that the ozone hole, PSC
173 occurrence and chlorine activation (more than a month, up to 2.2 ppbv) lasted longer in this year. An extensive
174 ozone hole from late August to mid-November is found in 2019. However, ozone increased after the minor
175 warming, and thus the ozone hole size (Fig. 3) and ozone loss reduced significantly thereafter (Fig. 4). The chlorine
176 activation was very strong and continuous from August to September (above 2.2 ppbv) in this year. Despite the
177 minor warming, the ozone loss in 2019 (3.0–3.4 ppmv) is similar to that in 2016. The nature of spring 2019 was
178 similar to the previous warm Antarctic years of 1988 and 2002, as the vortex was short-lived and highly variable

179 due to strong tropospheric forcing and SSW (Manney et al., 2020; Klekociuk et al., 2021). The peak ozone loss in
180 2019 is about 3.4 ppmv, which is higher than that in other winters, except 2020 (Wargan et al., 2020; Roy et al.,
181 2022). The chlorine activation remained at its peak value (2.0–2.2 ppbv) for several days in August before the peak
182 ozone loss in 2019, and the spatial distribution (450–550 K) of these high ClO values is the largest compared to all
183 other years. The 2020 ozone loss is very high (up to 3.6 ppmv) and exceeds the maximum ozone loss in other
184 winters. The chlorine activation rose in the early spring (September) (2.0–2.2 ppbv) and is similar to that in 2016.
185 The high values of ozone loss may have resulted from the increased aerosol loading from the Australian bushfires
186 in 2020 (e.g., Stone et al., 2021). A recent study by Ansmann et al. (2022) shows that about 10–20% of the ozone
187 loss in 2020 was driven by wildfire smoke by causing the growth of PSC particles.

188

189 **Interannual variability of ozone loss**

190

191 The interannual variability of ozone loss, PSC and chlorine activation is shown in Fig. 5. Here, the ozone loss is
192 computed by taking the averaged ozone loss from day 270 to 300 (the peak loss period) in the altitude range 450–
193 550 K (the peak loss altitudes, see Fig. 4). Similarly, the chlorine activation is indicated as the average of ClO over
194 the same altitude range, but for the days between 210 and 270. The weighted mean of the PSC area is shown with
195 black solid line for the years 2013–2020. Note that the peak ozone loss duration and altitude range are different in
196 different winters (e.g. 2018 and 2020). The smallest ozone loss is estimated for the years 2015 and 2017 because
197 of the relatively weak chlorine activation. The mean ozone loss is about 2.4 ppmv and ClO is about 1.75–1.95 ppbv
198 in both years. However, the PSC area in 2015 (11.9 million km²) was higher than most of other cold winters. The
199 larger PSC area is mostly because of the lower temperature conditions that lasted longer in the winter. Tully et al.
200 (2019) identified 2015 as one of the most severe and extreme winters, as also found in our study. The PSC area in
201 2017 (10.2 million km²) is smaller and therefore, ozone loss is lower as compared to that in 2015, which is
202 consistent with the results of Baarthen (2018).

203

204 The highest ozone loss is estimated in 2020 (3.1 ppmv) in the spring, which is followed by 2016 (3.0 ppmv). The
205 chlorine activation for both years is also higher than that of a few other cold winters, as scaled by ClO, about 2.1–
206 2.2 ppbv. The highest ozone loss in 2020 is favoured by the very large PSC area (12.6 million Km²). The 2018
207 spring was also unique in comparison to the other years as a consequence of the high chlorine activation (2.2 ppbv)
208 and very large PSC area (12.0 million Km²). The chlorine activation was very high in 2019 (2.1 ppbv), but the
209 relatively lower ozone loss during this particular period is a direct consequence of the unfavourable dynamic

210 condition (SSW). The PSC area is also lowest in 2019 (9.4 million Km²) among the winters due to SSW. The ozone
211 loss (2.7–2.8 ppmv) and chlorine activation (2.1–2.2 ppbv) are similar in other winters.

212

213 The ozone partial column loss at 350–750 K yields similar values for most winters, as the highest loss is estimated
214 for 2015, 2016, 2018 and 2019 (around 163±16 DU), consistent with the meteorology of the winters. However, the
215 lowest column loss (128±12 DU) is estimated for the winter 2020 here, as the vertical spread of ozone loss is limited
216 beyond the peak ozone loss altitude range of 450–550 K in this winter (see Fig. 4). Similarly, ozone loss in the
217 moderately cold winters show a loss of about 154±15 DU (2013 and 2014), but very small loss in 2017 (134±13
218 DU). The column loss computed at 400–600 K, the highest ozone loss altitudes in the Antarctic, has slightly lower
219 values as expected. In general, there is an average difference of about 40 DU (higher than the 400–600 K) ozone
220 loss between these altitude ranges (e.g., Kuttippurath et al., 2015). The loss is highest in 2019 (145±14 DU) at 400–
221 600 K as in the case of 350–750 K, but smallest in 2015 (107±10 DU). This suggests that there is higher ozone loss
222 at altitudes above 600 K in the very cold winter of 2015 (see Fig. 4). On the other hand, ozone loss and its difference
223 between these two altitude ranges are very small for 2020 and 2017, as discussed before.

224

225 **Conclusion**

226 We analyse the ozone loss for the past 8 years (2013–2020) in the Antarctic. The year 2019 had a warm winter
227 with a mW in mid-September. The winter of 2017 also showed similar characteristics, such as the sudden increase
228 in temperature during late August, higher minimum temperature (about 205 K) in August than in other years and
229 the sharp decrease in PSC area towards the end of September. The heat flux magnitude for the year (2017) is also
230 higher than the other winters (up to -60 Kms⁻¹), suggesting that it was a disturbed warm winter. We find a minimal
231 ozone loss in 2017 and it stayed less than 2.8 ppmv (110±11 DU at 400–600 K) for most of October and September.
232 Chlorine activation was also below 1.8 ppbv in August and September for the year. Conversely, the wave fluxes
233 are lowest in 2015. The temperature and PSC area follow similar temporal evolution in 2013, 2014, 2015, 2016
234 and 2018. Winter 2020 exhibits unique meteorology with a long-lasting occurrence of vortex-wide PSCs (12.6
235 million Km²) and thus, shows the highest ozone loss (3.5 ppmv). On the other hand, the lowest ozone loss (2.5
236 ppmv or 107±10 DU at 400–600 K) is estimated in 2015. Our study, thus, helps in understanding how the chlorine
237 activation and meteorology of the winters influence the variability of ozone. Dynamics and chemistry of the winters
238 play their respective roles in the ozone loss process. The winter of 2019 is an example of favourable chemistry
239 helping in increased ozone loss, though the dynamical conditions were unfavourable.

240 **Acknowledgements**

241 We thank the Indian Institute of Technology Kharagpur, for facilitating the study. We acknowledge free use of the
242 MLS data, which are taken from <https://disc.gsfc.nasa.gov/>. The meteorological data are acquired through
243 https://ozonewatch.gsfc.nasa.gov. The REPROBUS data are acquired through IPSL, <http://cds-espri.ipsl.fr/>. We
244 thank Cathy Boone for her help with the model runs, analyses and data transfer, and IPSL for hosting the data.

245

246 **Data availability**

247 The data used in this study are publicly available. The analysed data/codes can also be provided on request.

248 **Competing Interests**

249 JK is an Editor of Atmospheric Chemistry and Physics. Otherwise, no competing interests.

250

251 **Author Contributions**

252 JK conceived the idea, and JK and RR wrote the original manuscript. The manuscript was subsequently revised
253 with inputs from PK and FL. The model runs and model results were analyzed by FL. The data analyses and figures
254 made by RR and PK. All authors participated in discussions and made suggestions, which were considered for the
255 final draft.

256

257

258

259

260

261

262

263

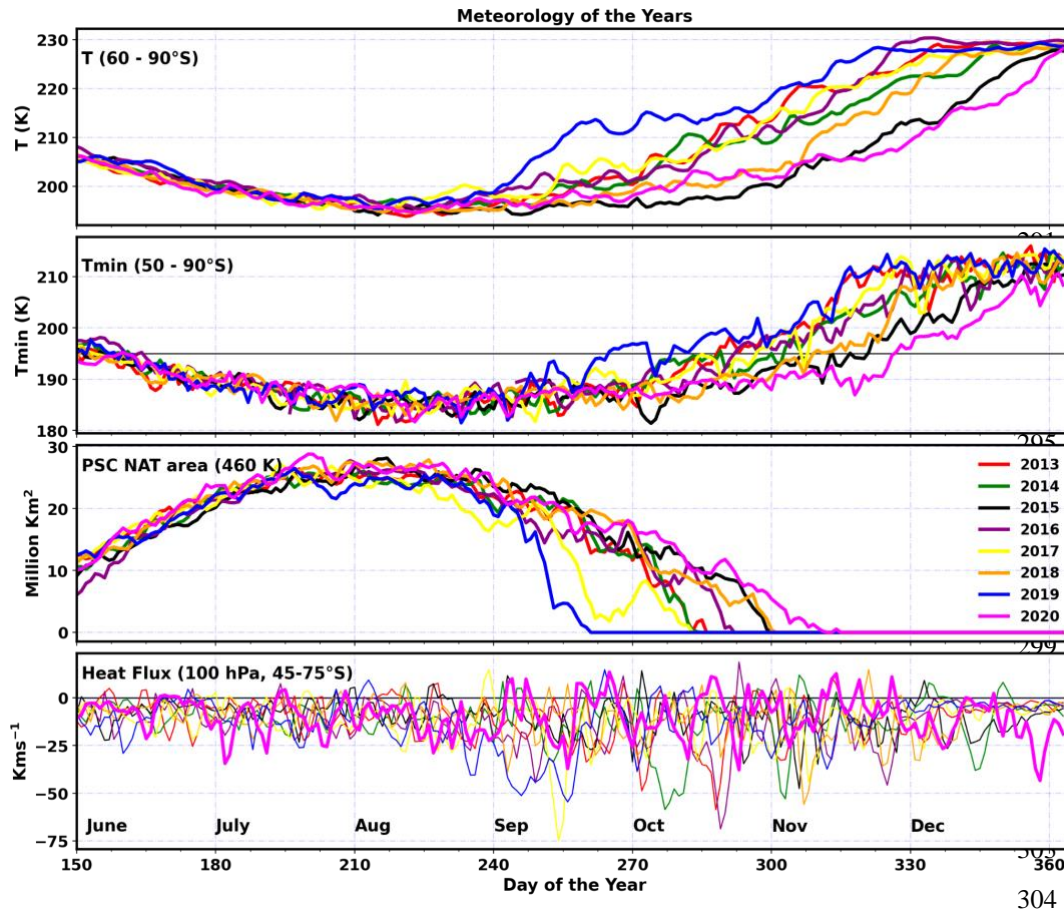
264

265 **Table 1:** The particle column ozone loss computed using the MLS ozone measurements and modelled passive
266 tracer by applying the passive method. The column loss is estimated for the peak ozone altitude ranges of 350–750
267 K and 400–600 K. The ozone column loss estimates have an uncertainty of about 10%.

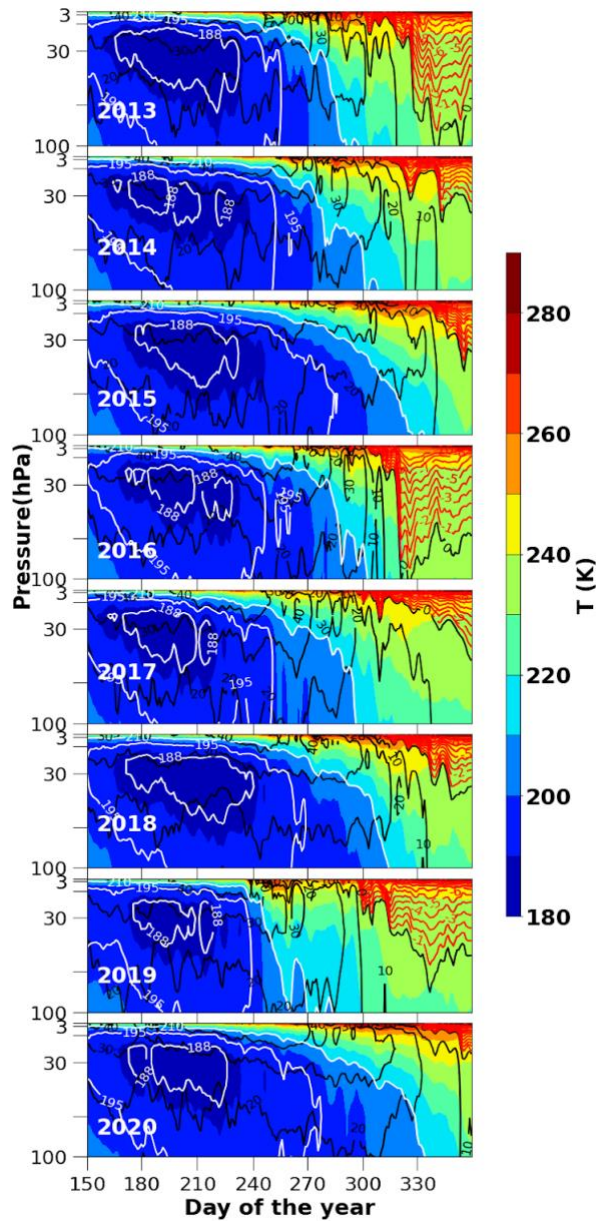
Year	Ozone column loss 350-750 K (DU)	Ozone column Loss 400-600 K (DU)
2013	153	122
2014	156	122
2015	169	107
2016	163	128
2017	134	110
2018	165	115
2019	169	145
2020	128	120

268
269
270
271
272
273
274
275
276
277
278
279
280
281
282
283

284
285



305 **Figure 1:** Meteorology of the years (2013–2020). Top panel shows the zonal average temperature (60° – 90° S) at
 306 100 hPa. Second panel (from top) shows the minimum temperature at 100 hPa. The black horizontal line in the
 307 panels shows 195 K (PSC formation threshold). Third panel (from top) shows the PSC area at 460 K and the bottom
 308 panel shows the mean heat flux (45° – 75° S) at 100 hPa. The black horizontal line in the bottom panel shows zero
 309 heat flux.
 310



311

312 **Figure 2:** Seasonal march of the zonal mean temperature for the period 2003–2020 averaged over the latitudes

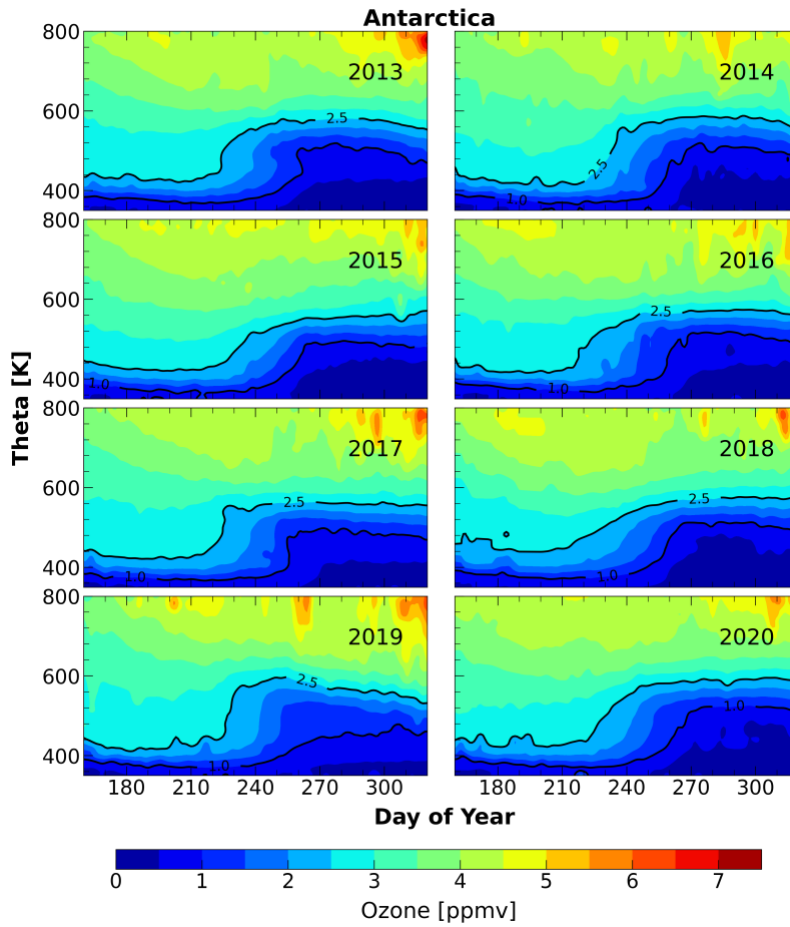
313 60°–90° S. The contours show the temperature and white contours represent specific temperatures such as 188, 195

314 and 210 K. The zonal wind velocities are overlaid. The black contour lines show the westerlies and the red contour

315 lines show the easterlies.

316

317



318
319

320 **Figure 3:** Temporal evolution of the vertical profiles of ozone averaged inside the vortex for the winters from
321 2013 to 2020 in the Antarctic. The temporal evolution is analysed using the MLS ozone data at 350–800 K for the
322 period June–November.

323

324

325

326

327

328

329

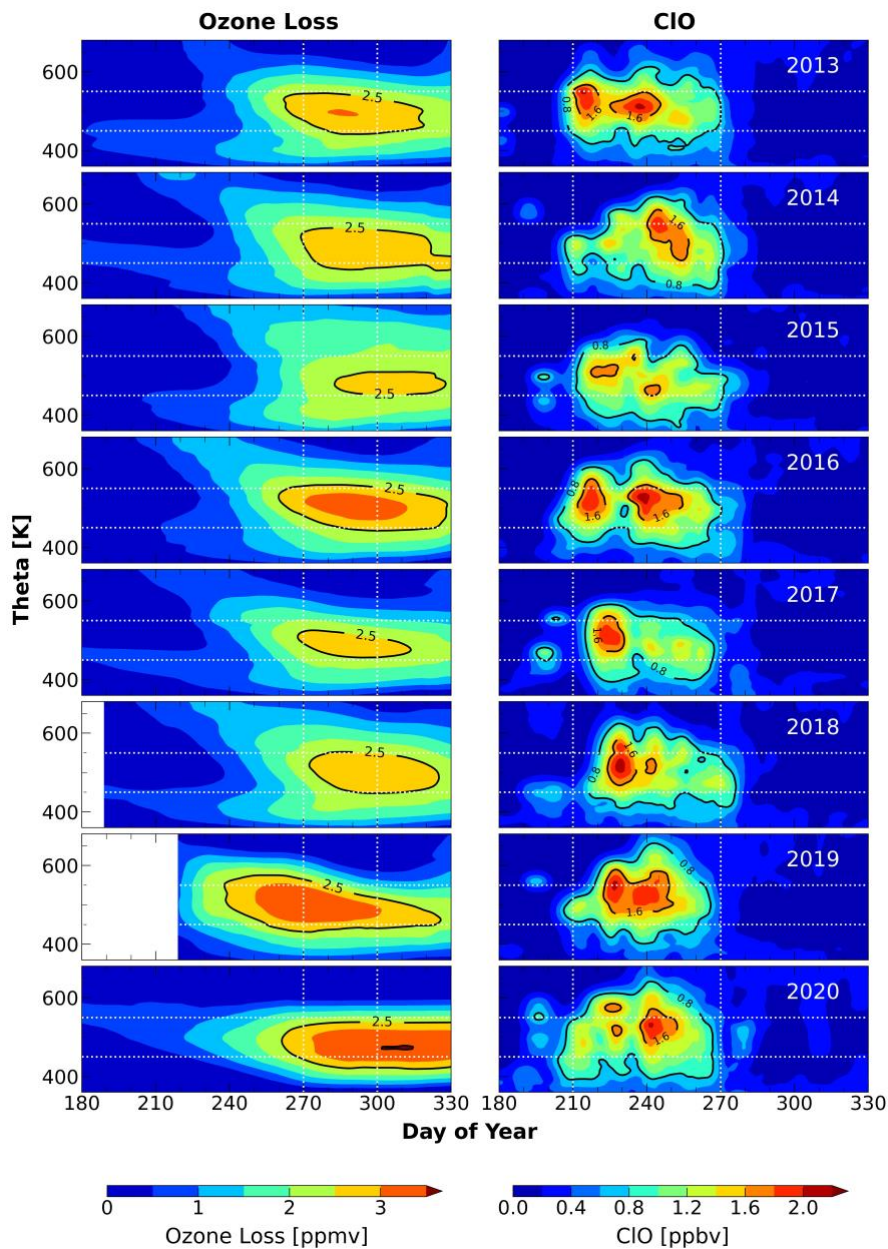
330

331

332

333

334

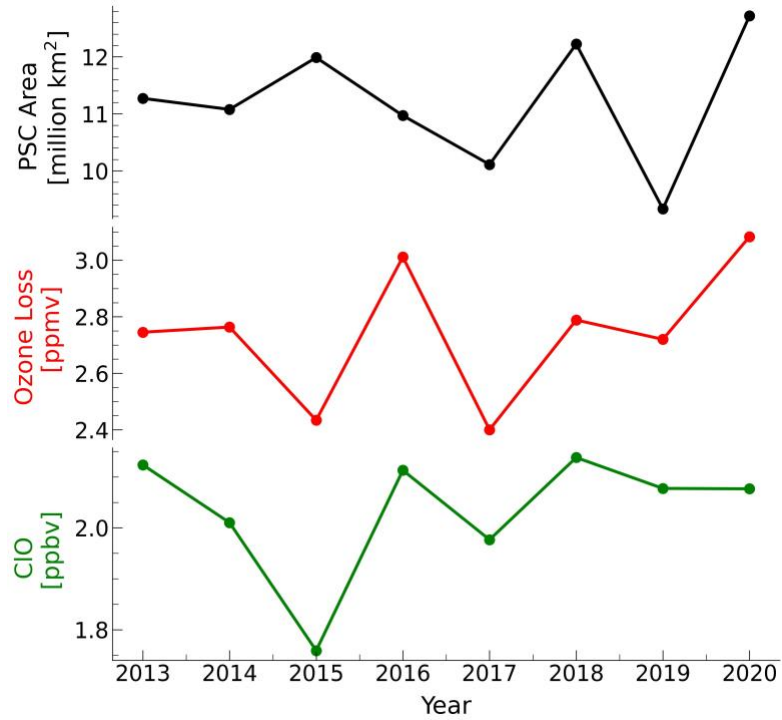


335
336
337
338
339

Figure 4: Temporal evolution of ozone loss estimated from MLS measurements using REPROBUS passive tracer (left). The MLS CIO measurements for the altitude range 350–700 K for the period 2013–2020 (right). The ozone loss estimates and CIO measurements are selected inside the polar vortex as per the Nash et al. (1996) criterion. Ozone loss is not computed up to 10 June 2018 and 20 July 2019 for not having tracer values.

340

341



342

343 **Figure 5:** The vortex-averaged ozone loss estimated from the MLS measurements using the passive method, peak
344 ClO measurements, and the weighted average of area of PSC for the period 2013–2020. The mean ozone loss is
345 estimated over the altitude range 450–550 K and between day 270 and 300 (maximum ozone loss days). The ClO
346 measurements are averaged over the altitude range 450–550 K and between day 210 and 270; representing the
347 strong chlorine activation period and altitudes.

348

349

350

351

352 **References**

- 353 Angell, J. K. and Free, M.: Ground-based observations of the slowdown in ozone decline and onset of ozone
354 increase, *J. Geophys. Res.*, 114, D07303, doi:10.1029/2008JD010860, 2009.
- 355 Ansmann, A., Ohneiser, K., Chudnovsky, A., Knopf, D. A., Eloranta, E. W., Villanueva, D., Seifert, P.,
356 Radenz, M., Barja, B., Zamorano, F., Jimenez, C., Engelmann, R., Baars, H., Griesche, H., Hofer, J.,
357 Althausen, D., and Wandinger, U.: Ozone depletion in the Arctic and Antarctic stratosphere induced by
358 wildfire smoke, *Atmos. Chem. Phys.*, 22, 11701–11726, <https://doi.org/10.5194/acp-22-11701-2022>, 2022.
- 359 Bandoro, J., Solomon, S., Donohoe, A., Thompson, D.W.J., and Santer, B.D.: Influences of the Antarctic ozone
360 hole on Southern Hemispheric summer climate change. *Journal of Climate*. 27(16):6245–6264. doi:
361 10.1175/JCLI-D-13-00698.1, 2014.
- 362 Braathen, G. O.: Observations of the Antarctic Ozone Hole from 2003 to 2017, p. 16503, 2018.
- 363 Butler, A., Daniel, J. S., Portmann, R. W., Ravishankara, A., Young, P. J., Fahey, D. W., and Rosenlof, K. H.:
364 Diverse policy implications for future ozone and surface UV in a changing climate, *Environ. Res. Lett.*, 11,
365 064 017, <https://doi.org/10.1088/1748-9326/11/6/064017>, 2016.
- 366 Chipperfield, M. P., Bekki, S., Dhomse, S., Harris, N. R., Hassler, B., Hossaini, R., Steinbrecht, W.,
367 Thiéblemont, R., and Weber, M.: Detecting recovery of the stratospheric ozone layer, *Nature*, 549, 211,
368 <https://doi.org/10.1038/nature23681>, 2017.
- 369 de Laat, A. T. J., van Weele, M., and van der A, R. J.: Onset of stratospheric ozone recovery in the Antarctic
370 ozone hole in assimilated daily total ozone columns, *J. Geophys. Res.-Atmos.*, 122,11880–11899,
371 <https://doi.org/10.1002/2016JD025723>, 2017.
- 372 Evtushevsky, O. M., Klekociuk, A. R., Kravchenko, V. O., Milinevsky, G. P., and Grytsai, A. V.: The influence
373 of large amplitude planetary waves on the Antarctic ozone hole of austral spring 2017. *J. South. Hemisph. Earth*
374 *Syst. Sci.*69, 57–64. doi:10.1071/ES19022, 2019.
- 375 Farman, J. C., B. G. Gardiner, and J. D. Shanklin.: Large losses of total ozone in Antarctica reveal seasonal
376 ClOx/NOx interaction, *Nature*, 315, 207-210, 1985.
- 377 Froidevaux, L., Jiang, Y. B., Lambert, A., Livesey, N. J., Read, W. G.; Waters, J. W., Browell, E. V., Hair, J. W.,
378 Avery, M. A., McGee, T. J., Twigg, L. W., Sunnicht, G. K., Jucks, K. W., Margitan, J. J., Sen, B., Stachnik, R.
379 A., Toon, G. C., Bernath, P. F., Boone, C. D., Walker, K. A., Filipiak, M. J., Harwood, R. S., Fuller, R. A.,
380 Manney, G. L., Schwartz, M. J., Daffer, W. H., Drouin, B. J., Cofield, R. E., Cuddy, D. T., Jarnot, R. F., Knosp,
381 B. W., Perun, V. S., Snyder, W. V., Stek, P. C., Thurstans, R. P., and Wagner, P. A.: Validation of Aura
382 Microwave Limb Sounder stratospheric ozone measurements. *J. Geophys. Res.* 113. 15-20.
383 10.1029/2007JD008771, 2008.
- 384 Gelaro, R., McCarty, W., Suárez, M. J., Todling, R., Molod, A., Takacs, L., Randles, C. A., Darmenov, A.,
385 Bosilovich, M. G., Reichle, R., Wargan, K., Coy, L., Cullather, R., Draper, C., Akella, S., Buchard, V., Conaty,
386 A., da Silva, A. M., Gu, W., Kim, G.-K., Koster, R., Lucchesi, R., Merkova, D., Nielsen, J. E., Partyka, G.,

387 Pawson, S., Putman, W., Rienecker, M., Schubert, S. D., Sienkiewicz, M., and Zhao, B.: The Modern-Era
388 Retrospective Analysis for Research and Applications, Version 2 (MERRA-2), *J. Climate*, 30, 5419–5454,
389 <https://doi.org/10.1175/JCLI-D-16-0758.1>, 2017.

390 Johnson, B. J., Cullis, P., Booth, J., Petropavlovskikh, I., McConville, G., Hassler, B., Morris, G. A., Sterling, C.,
391 and Oltmans, S.: South Pole Station ozonesondes: variability and trends in the springtime Antarctic ozone hole
392 1986–2021, *Atmos. Chem. Phys.*, 23, 3133–3146, <https://doi.org/10.5194/acp-23-3133-2023>, 2023.
393

394 Klekociuk, A.; Tully, MB; Krummel, PB; Evtushevsky, O; Kravchenko, V; Henderson, SI; et al.: The Antarctic
395 ozone hole during 2017. University Of Tasmania. Journal contribution.
396 <https://hdl.handle.net/102.100.100/558640>, 2020.

397 Klekociuk, A.R., M.B. Tully, P.B. Krummel, S.I. Henderson, D. Smale, R. Querel, S. Nichol, S.P. Alexander,
398 P.J. Fraser, and G. Nedoluha, The Antarctic ozone hole during 2018 and 2019, *J. South. Hemisphere Earth Syst.*
399 *Sci.*, 71, 66–91, doi:10.1071/ES20010, 2021

400 Krummel, P. B., Fraser, P. J., and Derek, N.: The 2015 Antarctic ozone hole and ozone science summary: final
401 report. (Report prepared for the Australian Government Department of the Environment, CSIRO:Australia.) iv,
402 27 pp, 2016.

403 Kuttippurath, J., Kumar, P., Nair, P. J., and Pandey, P. C.: Emergence of ozone recovery evidenced by reduction
404 in the occurrence of Antarctic ozone loss saturation. *Npj Climate and Atmospheric Science*, 1(1).
405 doi:10.1038/s41612-018-0052-6, 2018.

406 Kuttippurath, J., and Nair, P. J.: The signs of Antarctic ozone hole recovery. *Sci. Rep.*, 7, 585,
407 doi:10.1038/s41598-017-00722-7, 2017.

408 Kuttippurath, J., Godin-Beekmann, S., Lefèvre, F., Santee, M. L., Froidevaux, L., and Hauchecorne, A.:
409 Variability in Antarctic ozone loss in the last decade (2004–2013): high-resolution simulations compared to Aura
410 MLS observations, *Atmos. Chem. Phys.*, 15, 10385–10397, <https://doi.org/10.5194/acp-15-10385-2015>, 2015.

411 Langematz, U., and Kunze, M.: An update on dynamical changes in the Arctic and Antarctic stratospheric polar
412 vortices. *Clim Dyn* 27, 647–660. <https://doi.org/10.1007/s00382-006-0156-2>, 2006.

413 Lefèvre, F., Brasseur, G. P., Folkins, I., Smith, A. K., and Simon, P.: Chemistry of the 1991/1992 stratospheric
414 winter: three-dimensional model simulation, *J. Geophys. Res.*, 99, 8183–8195, 1994.

415 Livesey, N. J., Read, W. G., Froidevaux, L., Lambert, A., Man-ney, G. L., Pumphrey, H. C., Santee, M. L.,
416 Schwartz, M. J., Wang, S., Cofield, R. E., Cuddy, D. T., Fuller, R. A., Jarnot, R. F., Jiang, J. H., Knosp, B. W.,
417 Stek, P. C., Wagner, P. A., and Wu, D. L.: Earth Observing System (EOS) Aura Microwave Limb Sounder
418 (MLS) Version 3.3 and 3.4 Level 2 data quality and description document, JPL D-33509, Propulsion Laboratory
419 California Institute of Technology, Pasadena, California, USA, 1–164, 2013.

420

- 421 Manney, G. L., Livesey, N. J., Santee, M. L., Froidevaux, L., Lambert, A., Lawrence, Z. D., et al.: Record- low
422 Arctic stratospheric ozone in 2020: MLS observations of chemical processes and comparisons with previous
423 extreme winters. *Geophys. Res. Lett.*, 47, e2020GL089063. [https://doi.org/ 10.1029/2020GL089063](https://doi.org/10.1029/2020GL089063), 2020.
- 424 Milinevsky, G., Evtushevsky, O., Klekociuk, A., Wang, Y., Grytsai, A., Shulga, V., and Ivaniha, O.: Early
425 indications of anomalous behaviour in the 2019 spring ozone hole over Antarctica. *International Journal of*
426 *Remote Sensing*, 41(19), 7530–7540. <https://doi.org/10.1080/2150704X.2020.1763497>, 2020.
- 427 Müller, R., Tilmes, S., Konopka, P., Groß, J.-U., and Jost, H.-J.: Impact of mixing and chemical change on
428 ozone-tracer relations in the polar vortex, *Atmos. Chem. Phys.*, 5, 3139–3151, [https://doi.org/10.5194/acp-5-](https://doi.org/10.5194/acp-5-3139-2005)
429 3139-2005, 2005.
- 430 Nash, E. R., Newman, P. A., Rosenfield, J. E., and Schoeberl, M. R.: An objective determination of the polar
431 vortex using Ertel’s potential vorticity, *J. Geophys. Res.*, 101, 9471–9478, 1996.
- 432 Pazmiño, A., S. Godin-
433 Beekmann, A. Hauchecorne, C. Claud, S. Khaykin, F. Goutail, E. Wolfram, J. Salvador, and E. Quel.:
434 Multiple symptoms of total ozone recovery inside the Antarctic vortex during austral spring. *Atmos. Chem.*
435 *Phys.*, 18, 7557-7572, 2018.
- 436 Polvani, L. M., Previdi, M., England, M. R., Chiodo, G., and Smith, K. L.: Substantial twentieth-century Arctic
437 warming caused by ozone-depleting substances. *Nature Climate Change*, 10(2), 130–133.
438 <https://doi.org/10.1038/s41558-019-0677-4>, 2020.
- 439 Rowland, F. S., J. E. Spencer, and M. J. Molina.: Stratospheric formation and photolysis of chlorine nitrate, *J.*
440 *Phys. Chem.*, 80, 2711-2713, 1976.
- 441 Roy, R., Kuttippurath, J., Lefèvre, F. et al. The sudden stratospheric warming and chemical ozone loss in the
442 Antarctic winter 2019: comparison with the winters of 1988 and 2002. *Theor Appl Climatol* 149, 119–130.
443 <https://doi.org/10.1007/s00704-022-04031-6>, 2022
- 444 Salby, M., E. Titova, and L. Deschamps.: Rebound of Antarctic ozone. *Geophys. Res. Lett.*, 38, L09702,
445 [doi:10.1029/2011GL047266](https://doi.org/10.1029/2011GL047266), 2011.
- 446 Santee, M., MacKenzie, I. A., Manney, G., Chipperfield, M., Bernath, P. F., Walker, K. A., Boone, C. D.,
447 Froidevaux, L., Livesey, N., and Waters, J. W.: A study of stratospheric chlorine partitioning based on new
448 satellite measurements and modeling, *J. Geophys. Res.*, 113, D12307, [doi:10.1029/2007JD009057](https://doi.org/10.1029/2007JD009057), 2008.
- 449 Shen, X., Wang, L., and Osprey, S.: Tropospheric forcing of the 2019 Antarctic sudden stratospheric warming.
450 *Geophys. Res. Lett.*, 47, e2020GL089343. <https://doi.org/10.1029/2020GL089343>, 2020b.
- 451 Shen, X., Wang, L., and Osprey, S.: The Southern Hemisphere sudden stratospheric warming of September 2019.
452 *Science Bulletin.* [doi:10.1016/j.scib.2020.06.028](https://doi.org/10.1016/j.scib.2020.06.028), 2020.
- 453 Solomon, S., Ivy, D. J., Kinnison, D., Mills, M. J., Neely, R. R. III, and Schmidt, A.: Emergence of healing in the
454 Antarctic ozone layer. *Science*, 252(6296), 269–274. <https://doi.org/10.1126/science.aae006>, 2016.

- 455 Solomon, S.: Stratospheric ozone depletion: A review of concepts and history. *Reviews of Geophysics*, 37(3),
456 275–316. doi:10.1029/1999rg900008, 1999.
- 457 Solomon S, Haskins J, Ivy DJ, Min F.: Fundamental differences between Arctic and Antarctic ozone depletion.
458 *Proc Natl Acad Sci U S A*. 2014;111(17):6220-6225. doi:10.1073/pnas.1319307111,2014
- 459 Stolarski, R. S., and R. J. Cicerone.: Stratospheric chlorine: A possible sink for ozone, *Can. J. Chem.*, 52, 1610-
460 1615, 1974.
- 461 Stone, K. A., Solomon, S., Kinnison, D. E., and Mills, M. J.: On Recent Large Antarctic Ozone Holes and Ozone
462 Recovery Metrics, *Geophys. Res. Lett.*, 48, e2021GL095232, <https://doi.org/10.1029/2021GL095232>, 2021.
- 463 Strahan, S. E., and Douglass, A. R.: Decline in Antarctic ozone depletion and lower stratospheric chlorine
464 determined from Aura Microwave Limb Sounder observations. *Geophys. Res. Lett.*, , 45, 382– 390.
465 <https://doi.org/10.1002/2017GL074830>, 2018.
- 466 Tully, M. B., Klekociuk, A. R., Krummel, P. B., Gies, H. P., Alexander, S. P., Fraser, P. J., Henderson, S. I.,
467 Schofield, R., Shanklin, J. D., and Stone, K. A.: The Antarctic ozone hole during 2015 and 2016. *J. South.*
468 *Hemisphere Earth Syst. Sci.*, 69(1), 16. <https://doi.org/10.1071/es19021>, 2019.
- 469 Vargin, P.N., Nikiforova, M.P. and Zvyagintsev, A.M.: Variability of the Antarctic Ozone Anomaly in 2011–
470 2018. *Russ. Meteorol. Hydrol.* 45, 63–73. <https://doi.org/10.3103/S1068373920020016>, 2020.
- 471 Wargan, K., Weir, B., Manney, G. L., Cohn, S. E., and Livesey, N. J.: The anomalous 2019 Antarctic ozone hole
472 in the GEOS constituent data assimilation system with MLS observations *J. Geophys. Res.* 125 e2020JD033335.
473 <https://doi.org/10.1029/2020JD033335>, 2020.
- 474 Weatherhead, E. C., Reinsel, G. C., Tiao, G. C., Jackman, C. H., Bishop, L., Hollandsworth Frith, S. M., DeLuisi,
475 J., Keller, T., Oltmans, S. J., Fleming, E. L., Wuebbles, D. J., Kerr, J. B., Miller, A. J., Herman, J., McPeters, R.,
476 Nagatani, R. M., and Frederick, J. E.: Detecting the recovery of total column ozone. *J. Geophys. Res-Atmos*,
477 105(D17), 22201–22210. <https://doi.org/10.1029/2000JD900063>, 2000.
- 478 Wespes, C., Hurtmans, D., Chabrillat, S., Ronsmans, G., Clerbaux, C., and Coheur, P.-F.: Is the recovery of
479 stratospheric O₃ speeding up in the Southern Hemisphere? An evaluation from the first IASI decadal record
480 (2008–2017), *Atmos. Chem. Phys.*, 19, 14031–14056, <https://doi.org/10.5194/acp-19-14031-2019>, 2019.
- 481 Williamson, D. L. and Rasch, P. J.: Two-dimensional semi-Lagrangian transport with shape-preserving
482 interpolation, *Mon. Weather Rev.*, 117, 102–129, 1989.
- 483 WMO (World Meteorological Organization): Scientific Assessment of Ozone Depletion: 2006, Global Ozone
484 Research and Monitoring Project – Report No. 50, 572 pp., Geneva, 2007
- 485 WMO: Scientific Assessment of Ozone Depletion: 2014 Global Ozone Research and Monitoring Project Report,
486 World Meteorological Organization, Geneva, Switzerland, pp. 416, 2014.

- 487 World Meteorological Organization (WMO) (2015), WMO Antarctic Ozone Bulletins (2015). [Available at
488 www.wmo.int/pages/prog/arep/WMOAntarcticOzoneBulletins2015.html.]
- 489 Yamazaki, Y., Matthias, V., Miyoshi, Y., Stolle, C., Siddiqui, T., Kervalishvili, G., et al.: September 2019
490 Antarctic sudden stratospheric warming: Quasi-6-day wave burst and ionospheric effects. *Geophys. Res. Lett.*,
491 47, e2019GL086577. <https://doi.org/10.1029/2019GL086577>, 2020.
- 492 Yang, E.-S., Cunnold, D. M., Newchurch, M. J., Salawitch, R. J., McCormick, M. P., Russell, J. M., Zawodny, J.
493 M., and Oltmans, S. J.: First stage of Antarctic ozone recovery, *J. Geophys. Res.*, 113, D20308,
494 <https://doi.org/10.1029/2007JD009675>, 2008.
- 495 Zuev, V. and Savelieva, E.: The cause of the strengthening of the Antarctic polar vortex during October–
496 November periods. *J. Atmos. Solar-Terrestrial Phys.* 190, doi: 10.1016/j.jastp.2019.04.016, 2019.

497

498

499

500

501

502

503

504 **V06/JK/REV/14112023/1429**

505